

Morphodynamic Classification of Beaches in some parts of the Iranian Coasts

Maryam Shiea^{1*}, Azadeh Valipour²

^{1*}Caspian Climate Company, Mashhad, Iran; m.shiea@gmail.com

²Department of Marine Science and Technology, Jouybar Branch, Islamic Azad University, Jouybar, Iran; a.valipour@yahoo.com

ARTICLE INFO

Article History:

Received: 20 Nov. 2020

Accepted: 28 Aug. 2021

Keywords:

Wave-Dominated

Wave-Tide

Beach State

Iran

Dimensionless Fall Parameter

Relative Tide Range

ABSTRACT

This research investigates the morphodynamic classification of beaches of Iran according to the dimensionless fall parameter (Ω) and the relative tide range (RTR). According to RTR parameter, the southern Iranian coast (Hormozgan province) is mixed wave and tide and the northern Iranian coast (Mazandaran province) is wave-dominated. By using some schemes, the beach states in the north regions of the eastern and central parts of the Mazandaran province are dissipative and in the western part it is intermediate. Also, in the south section in most of the regions of the Hormozgan province, the beach states are ultradissipative, but in some areas low tide terrace and low tide bar/rip occur.

1. Introduction

Despite the long history of research on the classification of beach morphodynamics, coastal classification can be useful in providing a conceptual framework for studying coastal environments, as well as predicting coastal morphology [1]. On the other hand, the relationship between coastal morphology and coastal risks (coastal crises and natural hazards) such as rip currents (based on beach state) is still a matter of great importance for coastal engineers and geomorphologists [2, 3, 4]. In the past years, coastal studies and the classification of morphodynamics have been carried out on various coastlines of the world with the help of various methods such as field experiments, numerical modeling in a variety of morphodynamic models [5, 6, 7, 8] and long-term field observations using video monitoring techniques [9, 10, 11, 12, 13, 14, 15]. One of these studies is the Wright and Short [16] research that relied on dynamic shore-based factors based on a 6-year observation period from the Australian coast. For these wave-dominated beaches, they presented a beach classification scheme in which three main beach states were identified as dissipative, intermediate, and reflective states (Figure 1).

Masselink and Short [17] have also identified a number of distinct morphological states or stages associated with various wave and tide regimes. In fact, they propounded the classification of natural beaches on the basis of four physical constraints: modal

breaking wave height, modal breaking wave period, sediment characteristics of the upper beach face and mean spring tide range. These variables are quantified by two dimensionless parameters: the dimensionless fall velocity Ω and the relative tide range RTR [2]. Figure 2, is a simplified version of this kind of classification that consists of eight major beach types placed into three categories.

These different coastal models in this classification are defined using a dimensionless fall velocity parameter (DFVP), which was first proposed by Gourlay [18] and rewritten by Dean [19].

$$\Omega = H_b / W_s T \quad (1)$$

where H_b = breaker height (m), T = wave period (s), and W_s = sediment fall velocity (m/s). Reflective beach states are expected to occur when $\Omega < 1$, intermediate beaches when $1 < \Omega < 6$, and dissipative beaches when $\Omega > 6$.

Masselink and Short [17] developed an empirical model to simulate the tide-induced migration of hydrodynamic processes across a beach profile and used the relative tide range RTR:

$$RTR = \frac{TR}{H_b} \quad (2)$$

Where TR is the tide range (m) to quantify tidal effects.

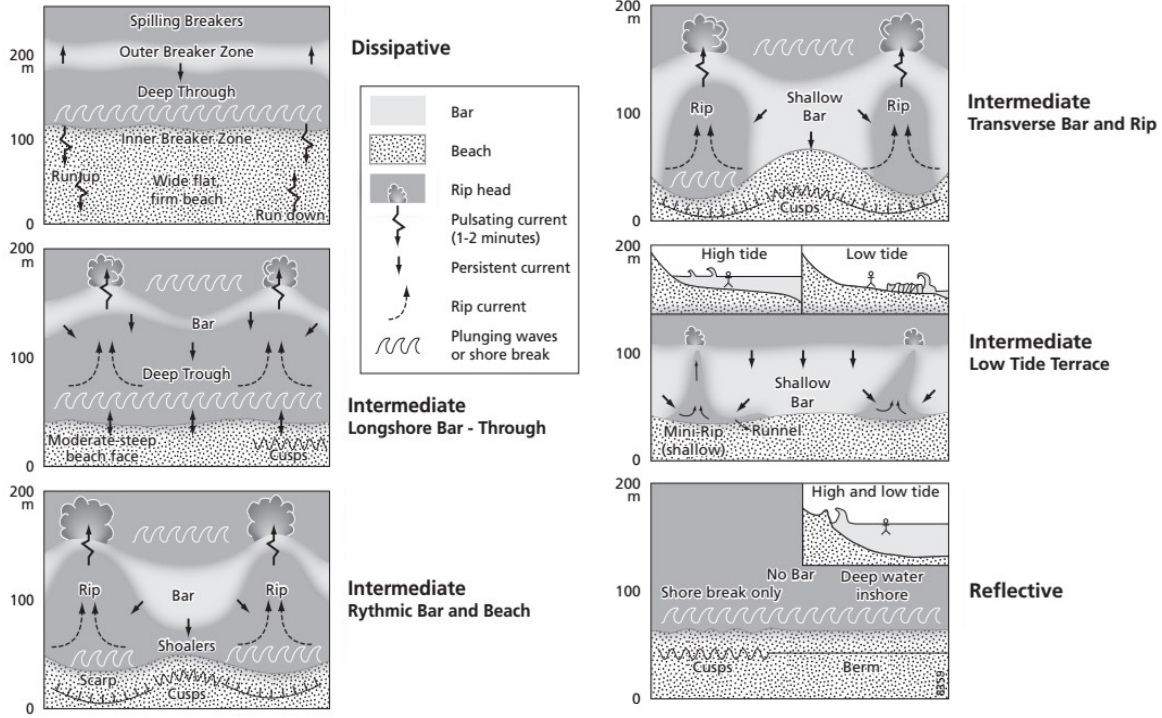


Figure 1. Plan and profile configurations of different kinds of wave-dominated beaches [2]

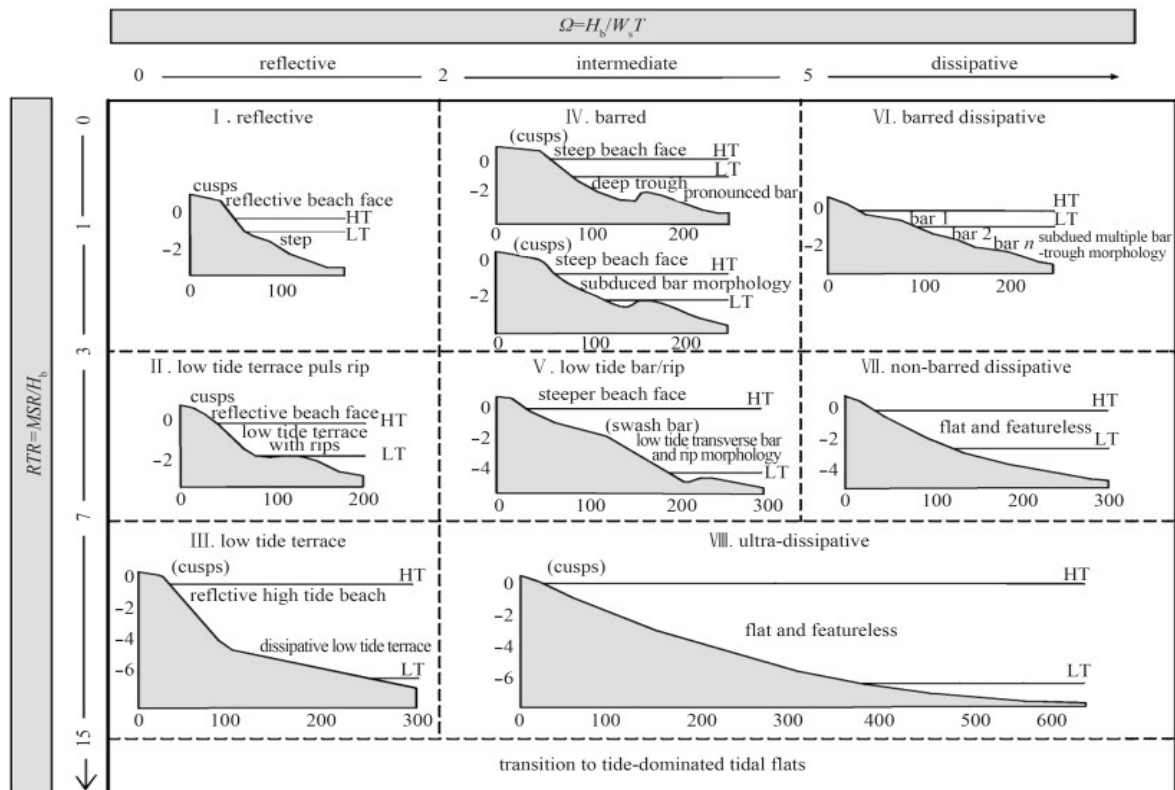


Figure 2. Conceptual beach model based on Ω and the relative tide range (RTR). When $RTR < 3$ and $\Omega < 2$. When $RTR > 3$ the transition to tide-dominated tidal flats is entered [17]

Also, Masselink and Hegge [20] studied the morphodynamic characteristics of three types of beach states by measurements of the morphology, waves, and longshore and cross-shore currents were conducted on two beaches on different macrotidal coastline of central Queensland (Australia). Summary

of morphodynamic characteristics of these types of beaches shows in Table 1. Short [21] presented Tide-modified and Tide dominated beaches models. Tide-modified beaches are divided into three states: Reflective +Low tide terrace (R+LTT), Reflective +Bars and Rips (R+LTR)

and Ultra-dissipative (UD). Also, Tide-dominated beaches are divided into three types: Beach +Sand riges (R+SR), Beach +Sand flats (R+SF) and Tidal Sand mud flats (RTSF).

The results of these studies showed that the morphological conditions and energy levels of the coast depend not only on the wave conditions but also on the range of tides and storms in each winter period. In Iran, few studies have been conducted on the classification of beaches, which can be pointed to the research carried out by Khoshnavan et al [22], based on sediments and geomorphologic evidence on the southern coasts of the Caspian Sea. Firoozfar et al[23] studied the changes of sea level on the southern coasts of the Caspian Sea by investigating the sediments and coastal profiles.

Rahbani et al [24] studied the south-eastern coastline of Iran (entrance of Coastal Makran) based on Shepard classification and using satellite imageries.

Kamranzad [25] investigated the wave characteristics in a 31-yearly period using localized ECMWF wind data and numerically model. The results of this study showed that the highest mean significant wave height occurs in the central strip of the middle parts of the Persian Gulf. While the monthly changes in wind and wave characteristics at different stations in the vicinity of the Strait of Hormuz is different.

Considering the mutual relationship between the beach states and the hydrodynamic and morphodynamic characteristics in beaches, determining the type of beach state in different regions of the northern and southern coastline of Iran plays an important role in the identification of characteristics of waves, currents, bed profile changes over time, coastal features and generally in the optimal coastal management of Iran. Therefore, in this study, beach states in some areas of the northern and southern coasts of Iran were classified according to the methods of Wright and Short [16] and Masselink and Hegge [20].

For this purpose, first the beaches' slope was estimated by using Arc GIS, then the breaker height and the tide range were calculated. Sediment features were characterized to estimate the dimensionless fall velocity and determine the beach state. Next, the role of waves, tides and sediments in formation of Iranian coast were studied.

The study is structured as follows: In section 2 different characteristics of the study area were described. In section 3 we presented data and methodology for determining the beach state in different stations. In section 4 the results were discussed by determining the hydrodynamic conditions and sediment characteristics. Also, spatial and seasonal changes in different coastal conditions were investigated and then the results of the studies were summarized in section 5.

2. Study area

The studied regions in this research include 14 stations located in the Caspian Sea coast in the Mazandaran Province (between $53^{\circ} 11' 34''$ E and $36^{\circ} 49' 54''$ N until $51^{\circ} 01' 30''$ E and $36^{\circ} 01' 0''$ N) and the Hormozgan province coast located near the Strait-of-Hormuz and the Persian Gulf (between $54^{\circ} 39' 18''$ E and $26^{\circ} 30' 29''$ N up to $53^{\circ} 9' 39''$ E and $27^{\circ} 4' 34''$ N). In Figure 3 and Table 2 the name and location of the study areas are presented.

Generally, there are no gravitational tides in the north Caspian basin, and only weak radiational tides are observed whereas a semidiurnal type of tide is predominant in the middle and south Caspian basins and maximum tidal range of 21 cm was found in the southeastern part of the Caspian Sea [26]. Caspian Sea coast can be classified into three areas based on onshore sediments: (1) sandy beaches: west Guilan, central Guilan, and east Mazandaran (2) gravelly beaches: west Mazandaran (in some segments; not the entire coastline) and (3) muddy beaches: Golestan province [23].

On the other hand, the Persian Gulf is a semi-enclosed, marginal sea that is exposed to an arid, sub-tropical climate. Tidal range varies from 3 to 3.4 meters in the northwest of Persian Gulf and decrease to 0.8 to 1.2 meters in western part of Hormozgan province also reaches to 2.7 to 3 meters in the extreme southeast. The Persian Gulf is located between latitudes 24° to 30° N, and is surrounded by deserts [27].

3. Data and methods

In order to achieve the research objectives, field observations and measurements, laboratory measurements and numerical model results, and finally computational methods, had been used. Field operations were done initially in two steps: (1) photography of the coastal features and important coastal phenomena (such as erosion cliffs, sand bars, channels of rip currents), (2) coastal sediment sampling. In the next step, the spatial variations of the coastal hydrodynamic and morphodynamic conditions in the northern and southern Iranian coasts were investigated by studying sediment variations, coastal features, and waves climate at each station.

Then, with regard to the characteristics of the waves and the calculation of the coastal slope, the calculation of sediment falls velocity (W_s), different beach states were determined in each station. The method for collecting morphological and hydrodynamic information at each of the stations on the northern and southern coasts is summarized in the table 3.

3.1. Wave breaker height

In this research the wave data from the modeling project (ISWM), which was done by the National Institute of Oceanography has been used. The patterns of wave breaking depend on the wave properties (wave height, wave period) and bed slope.

Table 1. Summary of morphodynamic characteristics of low tide terrace, low tide bar/rip and ultra-dissipative beaches [20]

Parameter/Process	Low Tide Terrace	Low Tide Bar/Rip	UltraDissipative
Ω	< 2(3)	2-5	>5(3)
RTR	3-15	3-7	3-15
High tide conditions and upper part of the intertidal profile			
Sediment size	>0.3 mm	0.2-0.4	<0.3
Tan β	>0.05	0.03-0.05	0.02-0.04
ϵ	<5	5-20	5-30
Breaker type	surging/plunging	Plunging	plunging/spilling
Attenuation coefficient	0.6-0.8	0.5-0.7	0.4-0.6
Dominant process	swash	swash/surf zone	swash/surf zone
Beach cusps	common	occasional	rare
Morphological change over lunar tidal cycle	Steepening during neap tides, flattening during spring tides	swash bar development, destruction and migration	minor, possible profile changes due to swash bar
Storm response	major erosion of steep upper part	erosion of upper part and of swash bar morphology	erosion upper part
Low tide conditions and lower part of the intertidal profile			
Sediment size	<0.2	<0.3	<0.2
Tan β	<0.03	0.02-0.04	<0.03
ϵ	>30	>20	>30
Breaker type	spilling	plunging/spilling	spilling
Attenuation coefficient	0.3-0.5	0.3-0.6	0.3-0.5
Dominant process	surf zone/shoaling	surf zone	surf zone/shoaling
Swash bars	occasional	Common	occasional
Rip currents	drainage rips at low tide	surf zone rips at low tide	absent
Tidal currents	important	minor importance	important
Morphological change over lunar tidal cycle	none	minor bar change	none
Storm response	deposition	deposition and destruction of bar morphology	deposition

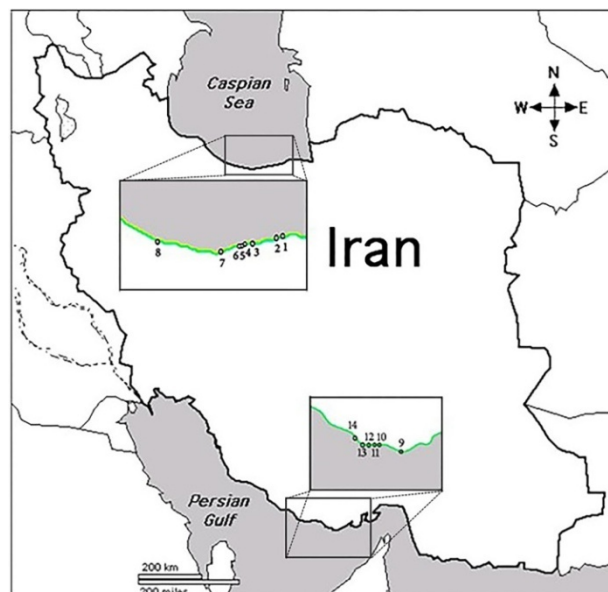


Figure 3. Map of Iran and locations of study areas and beach sites 1-14

Table 2. The names and locations of different stations in the study

NO.	Station name	Station location
Northern beaches		
1	Neka	Long:53° 11' 34" lat: 36° 49' 54"
2	Farahabad	Long:53° 03' 35" lat:36° 47' 57"
3	Larim	Long:52° 55' 48" lat: 36° 45' 53"
4	Naftchal	Long:52° 48' 06" lat: 36° 44' 16"
5	Mazandaran university	Long:52° 42' 04" lat: 36° 43' 19"
6	Babolsar	Long:52° 40' 06" lat: 36° 42' 57"
7	Noor	Long:52° 03' 29" lat: 36° 35' 09"
8	Nashtarud	Long:51° 01' 30" lat: 36° 01' 0"
Southern beaches		
9	Bostaneh	Long:54° 39' 18" lat:26° 30' 29"
10	Charak	Long:54° 3' 14" lat:26° 44' 27"
11	Gorzeh	Long:53° 53' 5" lat:26° 43' 22"
12	Near Gorzeh	Long:53° 51' 24" lat:26° 42' 23"
13	Chiruyeh	Long:53° 44' 4" lat:26° 42' 6"
14	Moghdan	Long:53° 9' 39" lat:27° 4' 34"

Weggel[28] based on some of experimental results proved the dependence of the breaking wave height on the bed slope as followed:

$$H = H_0 \left(\frac{C_0}{2nc} \right)^{\frac{1}{2}} \left(\frac{\cos \theta_0}{\cos \theta} \right)^{\frac{1}{2}} \quad (7)$$

$$K = b(m) - a(m) \frac{H_b}{gT^2} \quad (3)$$

where

$$a(m) = 43.8(1.0 - e^{-19m}) \quad (4)$$

$$b(m) = 1.56(1.0 - e^{-19.5m})^{-1} \quad (5)$$

In these relations, m is the beach slope, T is the wave period, and H_b is the breaking wave height. Also, McCowan [29] showed that waves break when their height becomes equal to a fraction of the water depth:

$$H_b = kd_b \quad (6)$$

As a first approximation, the breaking wave depth can be obtained if the characteristics of the offshore wave are known by shoaling and refraction formulas in the case of straight and parallel contours [30]

For shallow water, this relationship is approximately equal to:

$$H = H_0 \left(\frac{C_0}{2\sqrt{gd}} \right)^{\frac{1}{2}} \left(\frac{\cos \theta_0}{1} \right)^{\frac{1}{2}} \quad (8)$$

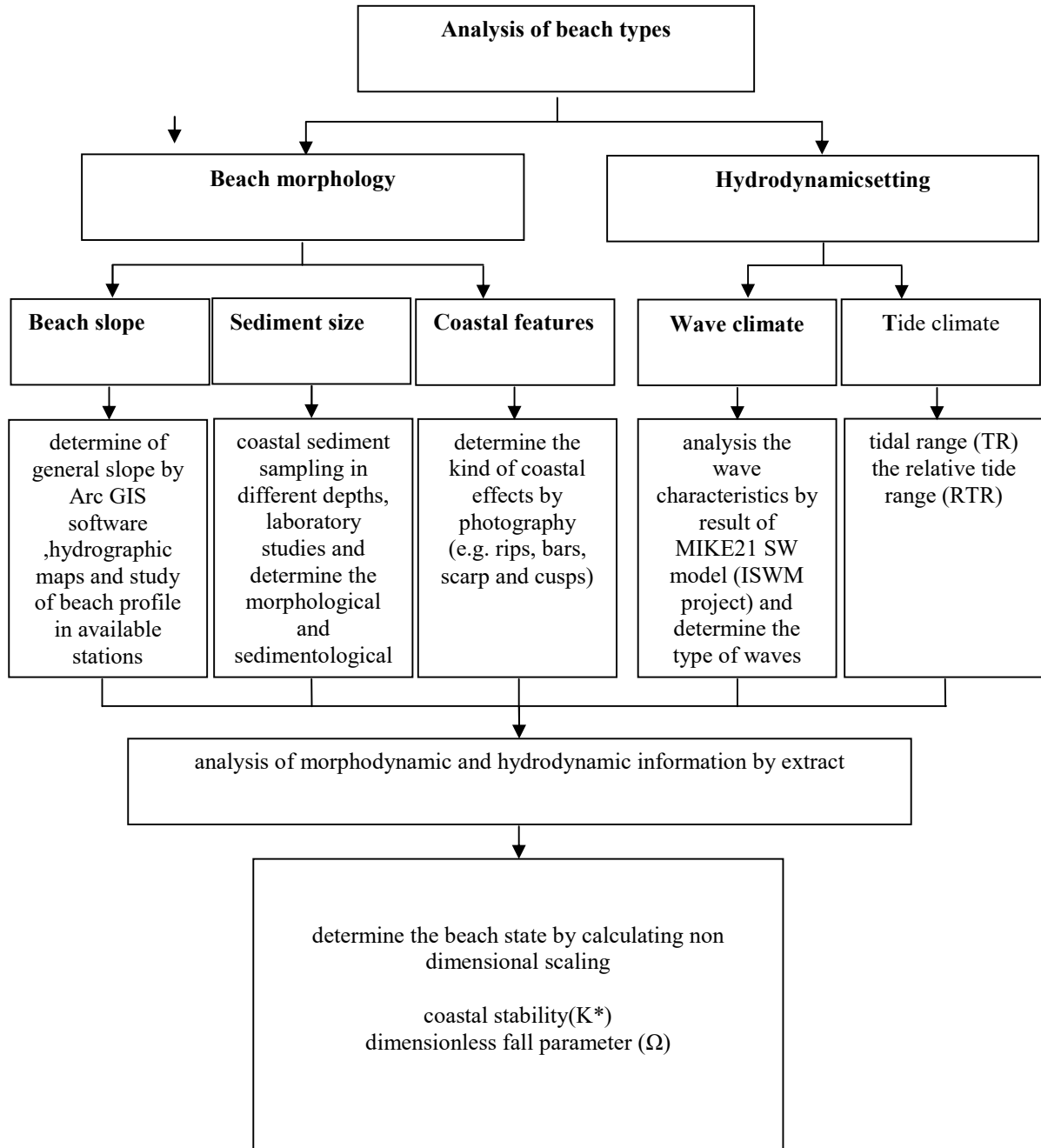
Now if the angle of wave breaking is assumed to be small ($\theta = 0$), we use the McCowan's breaking criterion:

$$Kd_b = H_0 \left[\frac{C_0}{2\sqrt{gd_b}} (\cos \theta_0) \right]^{\frac{1}{2}} \quad (9)$$

And so d_b can be written as:

$$d_b = \frac{1}{g^{\frac{1}{5}} k^{\frac{4}{5}}} \left(\frac{H_0 C_0 \cos \theta_0}{2} \right)^{\frac{2}{5}} \quad (10)$$

Table 3: Morphological and hydrodynamic information at each station on the northern and southern coast.



In the above relation H_0 is the average height of deep water, $C_0 = \frac{gT}{2\pi}$ is the velocity of the deep-water wave and θ_0 is the radiation angle of the dominant waves. The value of d_b obtained from the above equation is replaced in equation 6, and then the resulting H_b is compared with the numerical value of the hypothetical H_{bh} . It is necessary to determine the breaking wave height at each station. This operation is repeated consecutively to establish the relationship $H_b \cong H_{bh}$. Therefore, due to the implementation of such a trial-and-error method, the breaker index is calculated at each station.

Table 3 shows the characteristics and properties of waves in the northern and southern regions of Iran.

3.2 Sediment grain sizes

In order to investigate the effect of hydrodynamic conditions on sediment transport and bed form in the coastal zone, sediment sampling operations were performed at depths that covered the entire nearshore zone. A total of 56 sand samples were collected at 14 stations. Samples were taken from different depths (0, 2.5, 5 and 10 meters) of cross-shore profile with different morphological features such as beach face, surf domain, troughs and bars. Then sand samples were analyzed from different depths of the northern coasts in the Oceanographic laboratory and sedimentary information related to southern coasts in the Marine Geological Organization. In this way, specific gravity of sediment particles and diameter of

50% of sediments were determined from different depths then the average of these parameters were obtained from information about different depths. Finally, the average dimensionless fall velocity parameter and scale of morphodynamic features were determined and calculated in accordance with the sedimentation status of each station.

3.3 Beach morphology: Fieldmapping and imageinterpretation

In this study, with the help of images taken from coastal features in accordance with the characteristics of each beach state, comparing the features of different stations and monitoring the type of breaking wave, the morphological characteristics of the beach during the year were evaluated.

4. Results and discussion

Since tidal oscillations in the south Caspian basin are mainly caused by radiational effects and maximum tidal range is negligible in the central part of the southern Caspian, the effects of tides on the hydrodynamic conditions of the beach are ignored [26]. Also, the waves play an important role in this basin and so these coastal areas were considered as wave-dominated coast and the Wright and Short [16] method was used to determine the state of the northern coast in this study. On the other hand, in Iranian southern coastal areas, considering the effects of the tide on these coasts and the weak effects of waves compared to the northern coastal area, the Masselink and Short [17] classification was used.

4.1 Hydrodynamic conditions

According to figure 4, the information obtained from the wave roses showed that the prevailing wave direction over the western coast of Mazandaran province was northward; and in the central and eastern parts, was mostly northwest and wave height decreases from west to east. Therefore, on the western parts of the northern Iranian coast, hydrodynamic conditions were stronger than the central and eastern regions.

While on the southern Iranian coast, the wave characteristics at different stations in the vicinity of the strait of Hormuz are variable. Also, according to the definition of the Iribarren Number ε_b :

$$\varepsilon_b = \frac{\tan \beta}{[H_b/L_0]^{1/2}} \quad (11)$$

(where $\tan \beta$ is the beach gradient and H_b is breaker wave height, L is the water length and the subscripts $_0$ indicate deep water conditions) in all southern coast stations occur spilling breakers (Figure 5), while in the northern coast spilling breakers were often observed (Table 4). Although at station 8 (Nashtarud), surging breakers occur during in some periods (Figure 6).

4.2. Sediment characteristics

According to the information recorded in table 5 that show characteristics and properties of sediments, the mean sediment grain size increases discontinuously from east to west on the northern Iranian coasts. Also, morphodynamic conditions on the northern coasts showed the morphodynamic effects from station 1 to 7 are related to the dissipative state. On the other hand, the eastern parts of these coasts had low height berms, wide surf zone and low slope (compared with other coastal regions). The southern Iranian coasts did not follow a certain order, but in all of the stations in these coasts, the sediments consisted of more than 95% sand and less than 5% gravel.

4.3. Beach states

Due to the minimal effects of the tide in the Caspian Sea and the conditions mentioned about the waves, these coasts are considered wave-dominated ($RTR < 3$). In this condition, to determine the beach state in the stations located in these area two dimensionless parameters, fall velocity parameter Ω and coastal stability were examined [31].

$$K^* = \frac{H_b^2}{gT^2d_{50}} \quad (12)$$

Where d_{50} is the median sediment grain size, g is acceleration due to gravity, T is the wave period. According Figure 7, the coastal conditions at seven stations in this area (Neka, Farahabad, Larim, Naftchal, Mazandaran University, Babolsar, and Noor) on average during the year were dissipative (D), while at the Nashtarud station was on intermediate state (Figure 8).

Along Iranian southern beaches, the spring tide range was $TR \sim 0.8 - 1.13$ m, and the wave period and breaker height ranged from $T \sim 0.95 - 2.89$ and $H_b = 0.10 - 0.30$ m. As a result, RTR ranges from 3 to 12 and all the beaches along the Hormozgan western coast were a tide-modified (see Short, 2006) and remain in this state throughout the year (Figure 9).

4.3.1. Wave-Dominated beaches (Iranian northern beaches)

4.3.1.1. Spatial variation in beach conditions

The poor hydrodynamic conditions with average breaker height of $H_b \sim 0.585-0.772$ m during the year, the gentle slope and fine sediments $d_{50} \sim 0.116 - 0.158$ mm cause the beach state to be mostly on the dissipative state in the eastern and central area of the Caspian Sea coasts (from Neka to Noor). There were some similar morphodynamic features in almost all the seven dissipative stations which are in accordance with the value of Ω in each station had a different scale. Hence, the eastern coast of Mazandaran had lower berm levels and wider surf zone with a slope less than other the coastal areas.

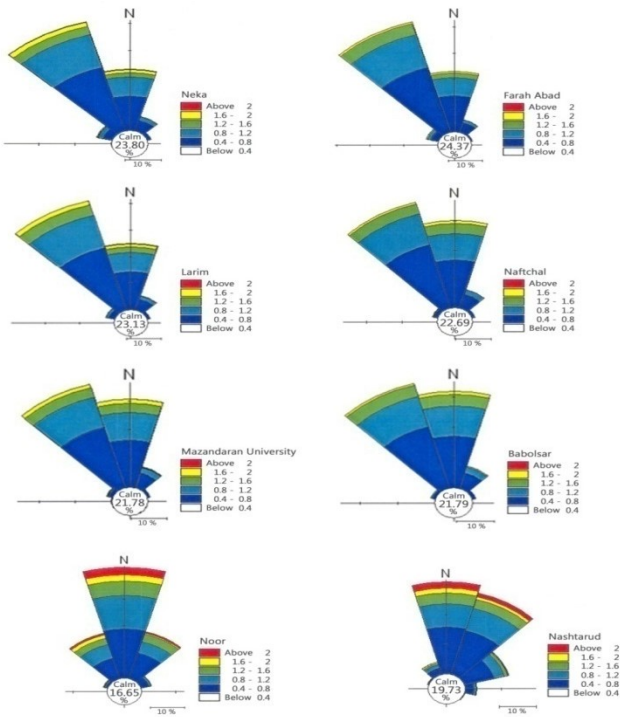


Figure 4. Wave rose of different stations of northern beaches

In the beaches that are not the fully dissipative state (all stations except for Naftchal), the crescentic bar was replaced shore-parallel sandbars when wave height decreased and these beaches were entered the intermediate state (RBB, LBT). Among these stations, there were more prominent bars and troughs in the bed of Noor and Farahabad stations. These sites also contained a mixture of undertow and rip currents system which changed in accordance with the prevailing morphodynamic conditions (Figure 10). While the beaches were fully dissipative state throughout the year (such as Naftchal) contained some subdued bars and troughs on the bed.

In the western stations such as Nashtarud with a steep slope in comparison with other stations (slope=0.0072), increasing the beach slope and stronger hydrodynamic conditions, especially increasing of sediment grain size had caused that this station was often on the intermediate (ridge-runnel or low tide terrace) during most of the year (85.2%) and beach profile was variable compared to other stations. Also, the type of breaker was predominantly spilling type ($\epsilon_b = 0.029$) in this station, but when the beach returned to the reflective state the probability of occurrence of the surging type increased (14.79%). compared to the eastern and central beach regions this beach entered the ridge-runnel state with narrow and weak rip currents during the year.

4.3.1.2. Seasonal variation in beach conditions

For the study of seasonal variation of the beach state in the northern stations, the changing procedure of coastal hydrodynamic and morphodynamic effects were investigated during the year.

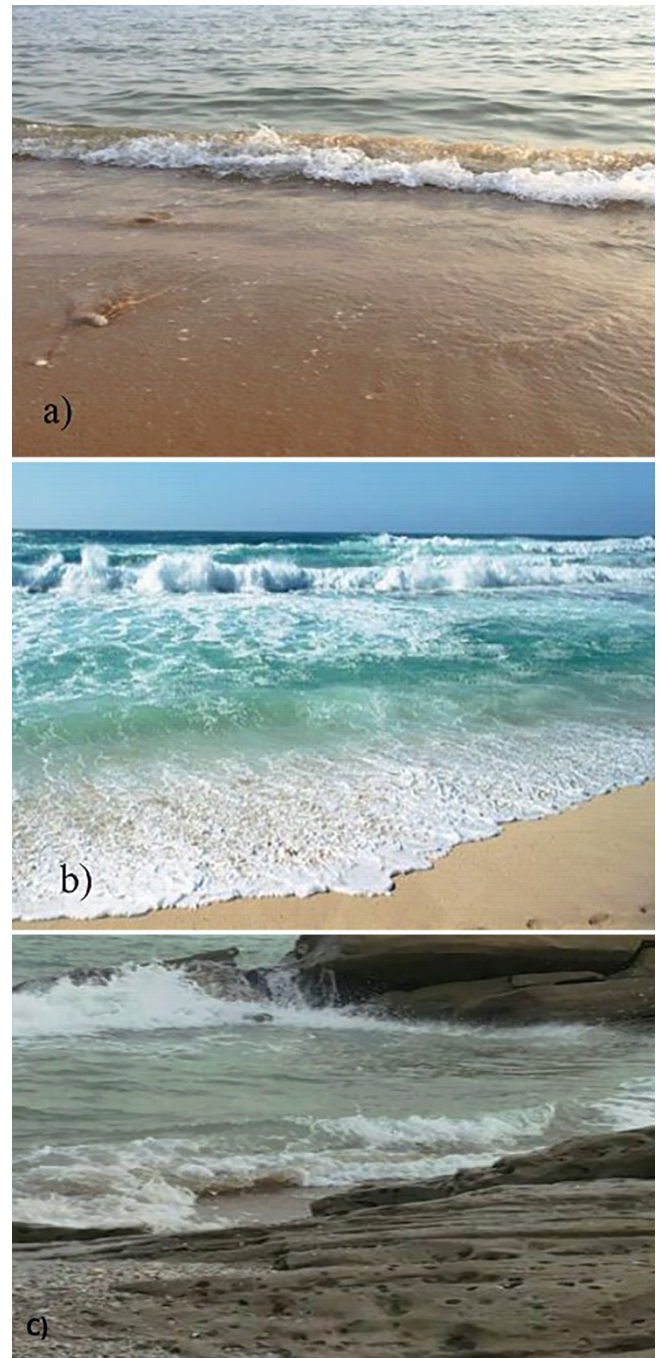


Figure 5. Spilling breakers at different stations on southern beaches a) Bostaneh (station 9) b) Charak (station 10) c) Moghdan (station 14)

According to Figure 11, diagram of the probabilities of annual occurrence of beach states for different stations of northern beaches showed that in all dissipative stations variations of beach state were small, so that the beach state was often in the dissipative state most of the year. But these changes were more evident in Nashtarud and regarding beach conditions had a good coordination with the intermediate beach state.

During winter when wave height increased, the profile of bed gradually changed as wave up rush and surf zone currents increased. These conditions also caused erosion and actually deepen of the rip channels. This process occurred while some bars sections were still

Table 3. Data of hydrodynamic properties of different stations in the study

NO.	Hs (m)	ε_b	T
Northern beaches			
1	1.128	0.018	2.69
2	1.093	0.023	2.68
3	1.131	0.025	2.69
4	1.125	0.026	2.69
5	1.14	0.024	2.71
6	1.17	0.021	2.74
7	1.375	0.042	2.98
8	1.312	0.029	2.91
Southern beaches			
9	0.487	0.018	2.897
10	0.254	0.179	1.717
11	0.168	0.056	0.956
12	0.223	0.090	1.226
13	0.273	0.013	2.480
14	0.281	0.013	1.494

connected to the beach. In this state, an increase in the height of the beach scarp was observed as the beach reached the transverse bar and rip (TBR) state. Given the severity of these rip currents when there were stormy conditions, the shoreline became more rhythmic. Based on field results, the beach state remained in this situation about 0.96% of the year (Nashtarud). Although this period was short, there was sufficient time for the beach to reach the transverse bar and beach (TBR) state. During summer wave height decreased gradually rip current velocity reduced and sediments moved from the bar to the beach. During this stage the surf zone width was reduced, the rip current channels were filled with sediment. So, the depth of the channels was reduced and the beach reached the ridge-runnell or low tide terrace (LTT) state, such that the rip currents became weak and the remaining narrow channels from these currents appeared as runnels on the beach profile. With the reduction of wave height and as more sediments transfer from the bars towards the beach, gradually all the runnels were filled with sediment and formed step-like effects in the base of the beach face. In this state the beach entered the reflective state (R). In general, the main impact on the beach profile was the bar connecting to the beach (terrace) and runnels. Other important effects in this area were the erosion scarps

which distance between the base of these scarps from the shoreline increased and the height reduces in warm seasons (Figure 12). This phenomenon is most likely related to beach state changes towards the reflective state and sea level changes.

4.3.2 Wave-Tide beaches (Iranian southern beaches)

4.3.2.1 Seasonal variation in beach conditions

According to Figure 13, generally in all the southern stations the effects of waves were stronger in spring and winter, so the highest wave effects were created in April, after that the wave height began to decrease and in October it was minimal.

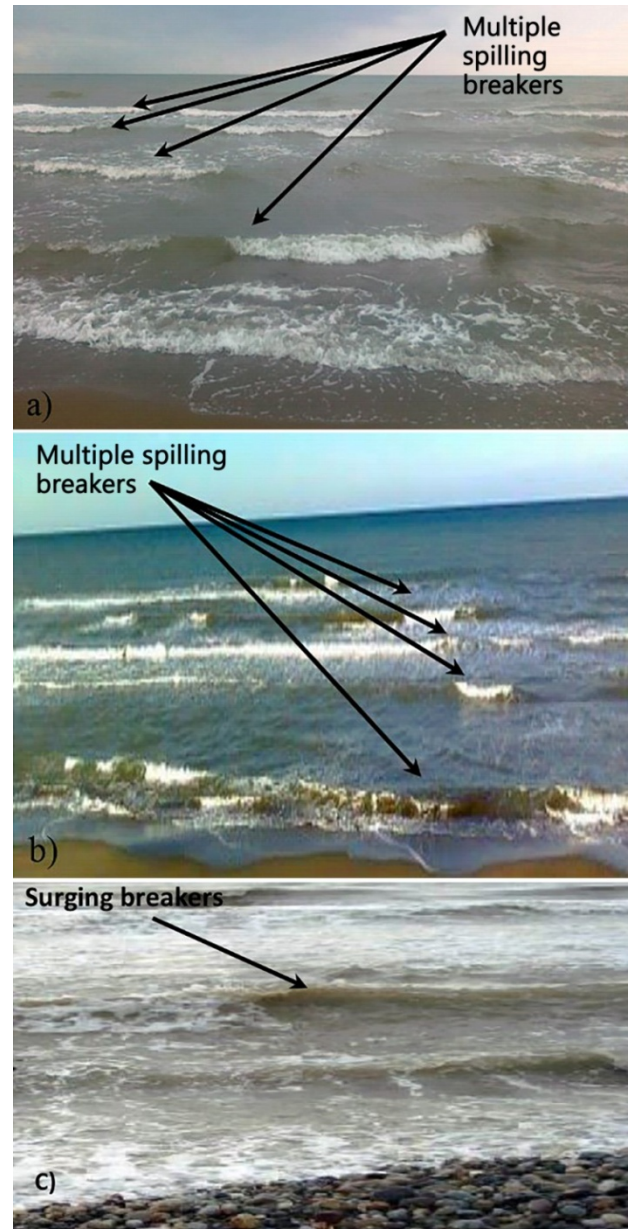


Figure 6. Breaker types on different stations in northern beaches a) Larim (station 3) b) Noor (station 7) c) Nashtarud (station 8)

Table 5. Sediment's characteristics of different stations in the study

NO.	D(ϕ)	d50(mm)	ρ (gr/cm ³)	w (m/s)
Northern beaches				
1	2.66	0.158	2.67	0.0182
2	2.64	0.116	2.67	0.0186
3	2.77	0.146	2.713	0.0169
4	2.96	0.128	2.71	0.013
5	2.76	0.147	2.72	0.0171
6	2.85	0.138	2.75	0.0154
7	2.10	0.23	2.71	0.028
8	0.95	1.93	2.71	0.187
Southern beaches				
9	1.577	0.25	2.1	0.0023
10	1.14	0.64	2	0.0603
11	1.752	0.215	2.85	0.0282
12	2.678	0.12	1.5	0.0035
13	2.723	0.115	2.5	0.0099
14	1.759	2.5	2.5	0.197

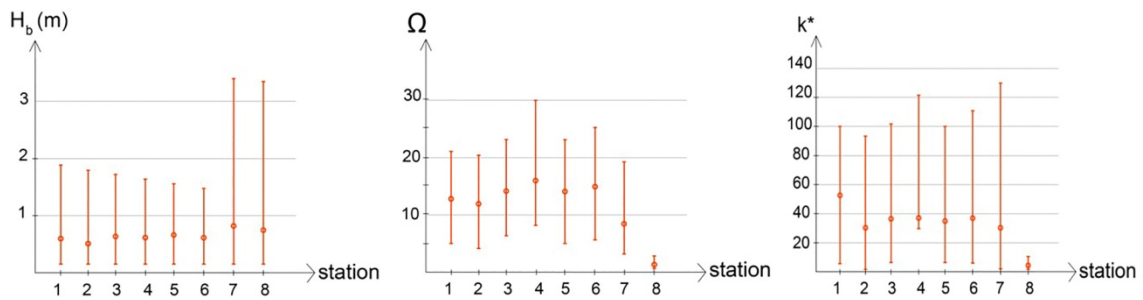


Figure 7. Range change of breaker height (H_b); sedimentation rate (Ω), coastal stability (k^*) and mean of these parameters (\bullet) at different stations of northern beaches



Figure 8. Examples of wave-dominated beaches in northern beaches a) Noor (station 7) b) Babolsar(station 6) c) Farahabad (station 2) d) Nashtarud (station 8)

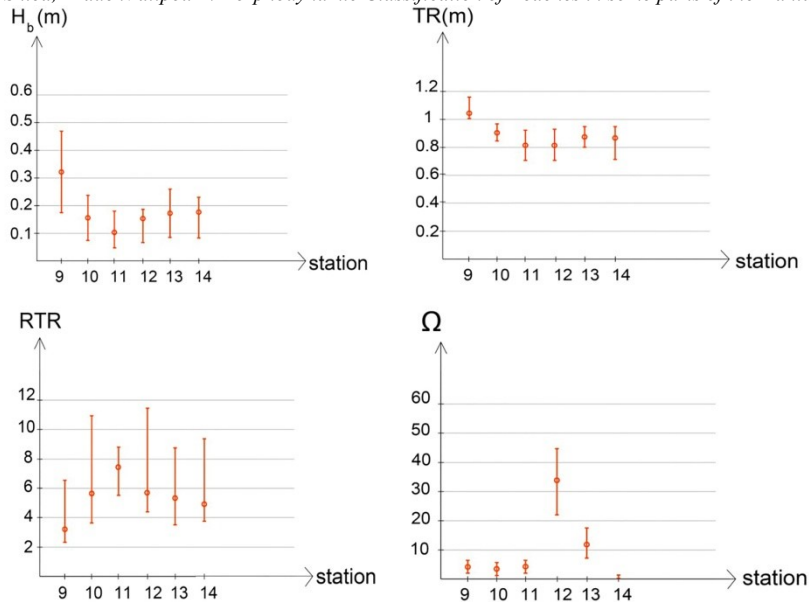


Figure 9. Range change of breaker height (H_b), tidal range (TR), relative tide range (RTR), sedimentation rate (Ω); mean of these parameters (•) at different stations of southern beaches



Figure 10. View of a topographic rip current and multiple longshore bar near Noor station

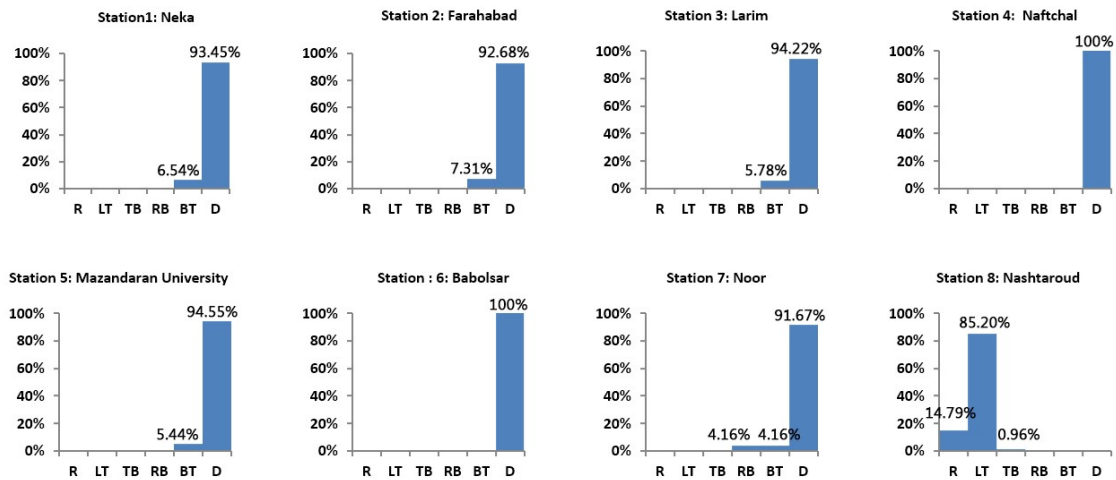


Figure 11. Probabilities of annual occurrence of beach states for different stations of northern beaches



Figure12. View of an erosion scarp at Nashtarud station

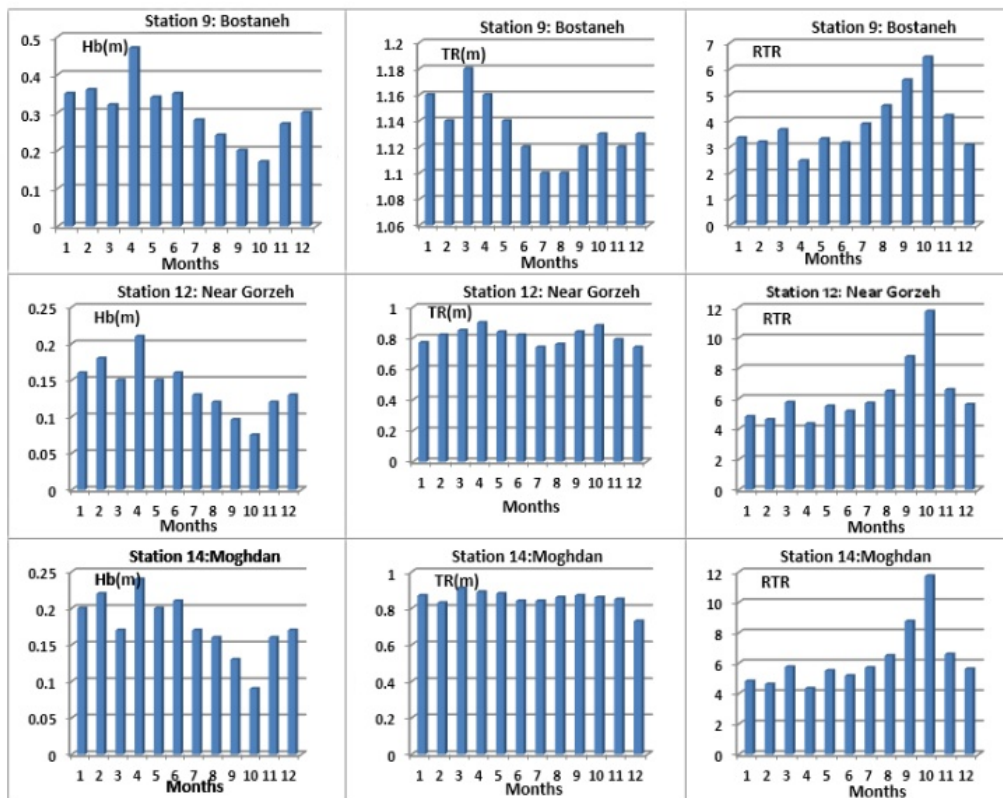


Figure13. Mean monthly of breaker height (H_b), tidal range (TR), relative tide range (RTR) during a year

On the other hand, tidal effects in fall and winter were at their maximum height. So that most amount of TR was observed in March. After March, tidal range decreased and in summer it was at its minimum, reaching its lowest in July (Figure 14).

Also, the study of the patterns' sediment grain size in all stations of the southern coast revealed that the sediment grain size did not follow a certain order.

However, despite the changes of tide and waves, the beach state for each station was almost fixed and unchangeable during the year.

4.3.2.2. Spatial variation in beach conditions

The results show that station 9 had the lowest slope (0.00277) and highest waves based on Figure 9 (H_b~0.175-0.47). Also, the intertidal sediment was 4.7% gravel and 95.3% sand. The average beach state during the year was low tide bar/rip beaches (75%), while 25% of the year the beach in this area was ultra-dissipative state.

At stations 10 and 14, the sediment particle diameter (in the upper part of the intertidal profile) was coarse

sand (0.64 mm) in station 10 and (very coarse sand) 2.5 mm in station 14 and this included 99.7% sand and 0.25% gravel. In these two stations the average beach state during the year was low tide terrace (92% at station 10) and became close to ultra-dissipative 8% of the year. However, at station 14 this state remained unchanged during the year, with the yearly incidence 100% low tide terrace (Figure 14).

In the three stations (11-13) located between Gorzeh and Chirooyeh Ports, the average beach state during the year was ultradissipative. This was primarily a result of the finer sediment (station 11 with $d_{50}=0.215$ mm, station 12 with $d_{50}=0.12$ mm and station 13 with $d_{50}=0.115$ mm) together with the relative tide range (RTR = 5-7), sedimentation rate ($\Omega = 5-35$) and the slope of these beaches was less than 0.03.

In station 11, close to the Gorzeh area ultradissipative conditions occurred 75% of the time and low-tide bar/rip 25% of the time, while at station 12 and 13 ultra-dissipative conditions prevails 100%.

5. Conclusion

The northern coasts of Iran are adjacent to the Caspian Sea, the largest lake in the world, and are exposed to short waves that increase in height from east to west. The waves combined with the minimum of tidal amplitudes in this region, result in wave-dominated beaches. In the southern regions of Iran, which borders the Persian Gulf, the waves are lower compared to the northern region of Iran and the presence of tides effects in these beaches cause them to be tide-modified. These differences of hydrodynamic factors cause a variety of beach states in the northern and southern coastal areas of Iran.

Results of this study show that for the northern beaches, 10 out of 11 stations are in the dissipative state while Nashtarod (station 8) is in the intermediate state (ridge-runnel or low tide terrace). By comparing the stations studied, it can be stated that, the most dissipative state can be observed in the Naftchal station and the least dissipative can be observed in the Noor and Farahabad stations. Also, there are very minimal changes during the year in the beaches in the stations in the dissipative state and so those beaches are in the dissipative state more than 90% of the year, while the intermediate beach ranges seasonally from reflective to transverse bar and rip.

On the southern beaches of Iran, a wide range of beach states are present in the study area: reflective, dissipative, and intermediate have been observed. However, the ultra-dissipative beaches (which are a part of the dissipative groups) at most of the stations undergo little annual change, while the stations with intermediate beach states such as low tide terrace beaches and or those with a bar, change during the year and can become close to the dissipative beach state. Based on the results of this study the most frequent beach states in the north and south of Iran are

dissipative, with the southern coastal area being tide-modified with the ultra-dissipative state.

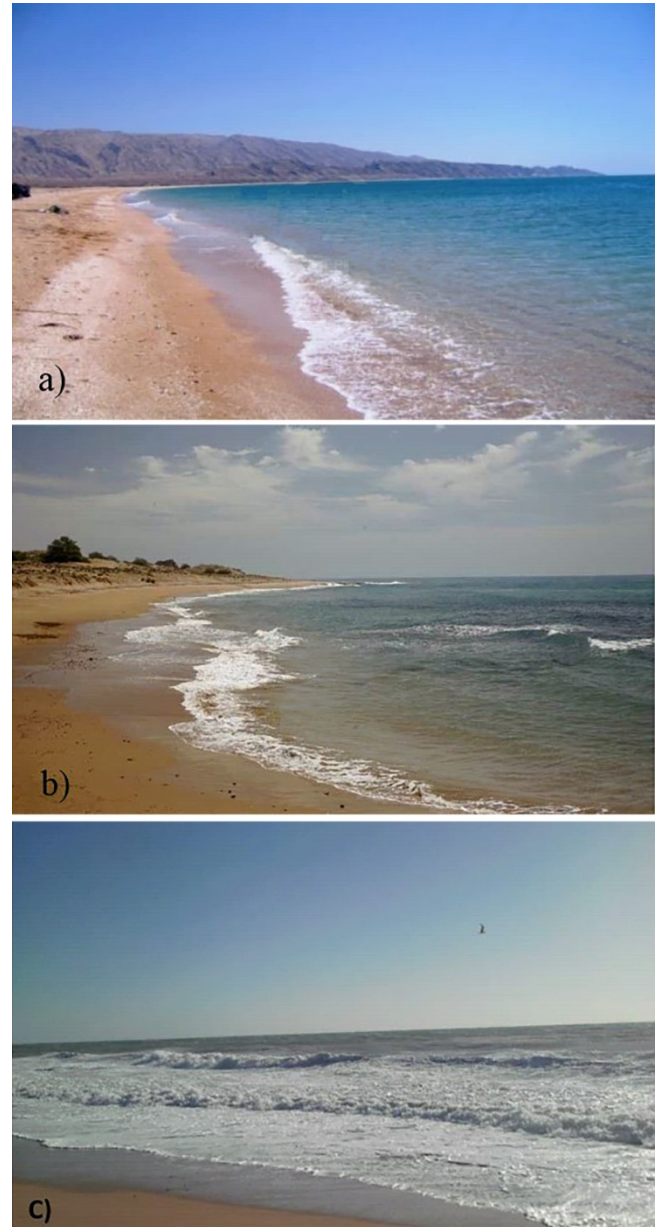


Figure 14. Examples of Wave-tide beaches in southern beaches a) Chiruyeh (station 13) b) Moghdan (station 14) c) Bostaneh (station 9)

are in the dissipative state more than 90% of the year, while the intermediate beach ranges seasonally from reflective to transverse bar and rip.

On the southern beaches of Iran, a wide range of beach states are present in the study area: reflective, dissipative, and intermediate have been observed. However, the ultra-dissipative beaches (which are a part of the dissipative groups) at most of the stations undergo little annual change, while the stations with intermediate beach states such as low tide terrace beaches and or those with a bar, change during the year and can become close to the dissipative beach state. Based on the results of this study the most frequent beach states in the north and south of Iran are

dissipative, with the southern coastal area being tide-modified with the ultra-dissipative state.

Acknowledgments

We are grateful to Professor A. Short for fruitful suggestions and valuable remarks. We would like to thank the Department of Physical Oceanography of the Iranian National Institute for Oceanography and Atmospheric Science (INIO) for providing wave and sediment data of the Mazandaran Province. In addition, we acknowledge the help of Dr. R. Lak from the Marine Geological Organization, Tehran, who provided us with the sediment data of the Hormozgan Province coast.

List of Symbols (Optional)

C_0	velocity of the deep water[m/s]
d_b	breaking wave depth [m]
d_{50}	median sediment grain size [mm]
g	acceleration due to gravity[m/s]
H_b	breaker height[m]
K^*	Coastal stability
L	water length[m]
m	beach slope
RTR	relative tide range
T	wave period [s]
TR	tide range [m]
W_s	sediment fall velocity [m/s]
θ_0	radiation angle
Ω	dimensionless fall velocity
ε_b	Iribarren Number

6. References

- 1-Scott, T., Masselink, G.y., Russel, P., (2011), *Morphodynamic characteristics and classification of beaches in England and Wales*, Marine Geology, Vol.286, p.1-20.
- 2- Short, A.D., (1999), *Beach and Shoreface Morphodynamics*, Chichester, United Kingdom: Wiley, p.379.
- 3-Short, A.D. and Hogan, C.L., (1994), *Rip currents and beach hazards: Their impact on public safety and implications for coastal management*, Journal Coastal Research, Special Issue No. 12, p.197-209.
- 4- Scott, T.M., Russell, P., Masselink, G. and Woolers, A., (2009), *Rip current variability and hazard along macro-tidal coast*, Journal of Coastal Research, SI 56, p.895–898.
- 5- Reniers, A.J.H.M., Roelvink, J.A., Thornton, E.B., (2004), *Morphodynamic modeling of an embayed beach under wave group forcing*, Journal of Geophysical Research, Vol.109, C01030. doi:10.1029/2002JC001586.
- 6- Garnier, R., Calvete, D., Falqués, A., and Caballeria, M., (2006), *Generation and nonlinear*

- evolution of shore-oblique/transverse sand bars*, Journal of Fluid Mechanics, Vol. 567, p.327–360.
- 7- Dronen, N., and Deigaard, R., (2007), *Quasi-three-dimensional modelling of the morphology of longshore bars*, Coastal Eng, Vol.54, p.197–215.
- 8- Smit, M.W.J., Reniers, A.J.H.M., Ruessink, B.G., Roelvink, J.A., (2008), *The morphological response of a nearshore double sandbar system to constant wave forcing*, Coastal Engineering, Vol.55, p.761–770.
- 9- Van Enckevort, I.M.J. and Ruessink, B.G., (2003a), *Video observations of nearshore bar behaviour. part 1: alongshore uniform variability*, Continental Shelf Research, Vol.23, p.501–512.
- 10- Van Enckevort, I.M.J. and Ruessink, B.G., (2003b), *Video observations of nearshore bar behaviour. part 2: alongshore non-uniform variability*, Continental Shelf Research, Vol.23, p.513–532.
- 11- Ranasinghe, R.; Symonds, G.; Black, K. and Holman, R.A., (2004), *Morphodynamics of intermediate beaches: a video imaging and numerical modelling study*, Coastal Engineering, Vol.51, p.629-655.
- 12- Quartel, S., Ruessink, B.G., Kroon, A., (2007), *Daily to seasonal cross-shore behaviour of quasi-persistent intertidal beach morphology*, Earth Surface Processes and Landforms, Vol.32, p.1293–1307.
- 13- Holland, K.T., Holman, R.A., Lippmann, T. C., Stanley, J and Plant, N., (1997), *Practical use of video imagery in nearshore oceanographic field studies*, Journal Oceanic Engineering, Vol.22(1), p.81-92.
- 14-Smit, M.W.J., Aarninkhof, S.G.J., Wijnberg, K.M., González, M., Kingston, K.S., Southgate, H.N., Ruessink, B.G., Holman, R.A., Siegle, E., Davidson, M., Medina, R., (2007), *The role of video imagery in predicting daily to monthly coastal evolution*, Coastal Engineering, Vol.54, p.539–553.
- 15- Klein, A.H.F. and de Menezes, J.T., (2001), *Beach morphodynamic and profile sequence for a headland bay coast*, Journal of Coastal Research, Vol.17, p.812–835.
- 16- Wright, L.D. and Short, A.D., (1984), *Morphodynamic variability of surf zones and beaches: A synthesis*, Marine Geology, Vol.56, p.93–118.
- 17- Masselink, G. and Short, A.D., (1993), *The effect of tide range on beach morphodynamics and morphology: a conceptual model*, Journal of Coastal Research, Vol.9(3), p.785–800.
- 18- GOURLAY, M.R., (1968), *Beach and Dune Erosion Tests*, Delft Hydraulics Laboratory Report M93 51M936, Delft.
- 19- Dean, R.G., (1973), *Heuristic models of sand transport in the surf zone*, Proc. Conf. Engineering Dynamics in the Surf Zone, Sydney, N.S.W, p.208–214.
- 20- Masselink, G. and Hegge, B., (1995), *Morphodynamics of meso- and macrotidal beaches:*

Examples from central Queensland, Australia, Marine Geology, Vol.129, p.1–23.

21- Short, A.D, (2006), *Australian beach systems – Nature and distribution*, Journal of Coastal Research, Vol.22(1), p.11-27.

22- Khoshravan, H., Rohanizadeh, S., Malek, J., Nejadgholi, G., (2011), *Caspian Sea southern coasts zoning on the basis of sedimentary morphodynamic indicators*, Journal of the Earth and Space Physics, Vol. 37(3), p.1-15 (in Persian).

23- Firoozfar, A., Bromhead, E.N., Dykes, A.P., and Neshaei, M.L., (2012), *Southern Caspian Sea Coasts, Morphology, Sediment Characteristics, and Sea Level Change*, Proceedings of the Annual International Conference on Soils, Sediments, Water and Energy, Vol. 17, Article 12, p.123-150.

24- Rahbani, M. and Pakhirehzan, M., (2018), *Classifying east coasts of Hormozgan province using Shepard method and satellite imagery*, The Egyptian Journal of Remote Sensing and Space Sciences, Vol.21, p.335-344.

25- Kamranzad, B., (2018), *Persian Gulf zone classification based on the wind and wave climate variability*, Ocean Engineering, Vol.169, p.604-635.

26- Medvedev, I.P., Kulikov, E.A., Rabinovich, A.B., (2017), *Tidal oscillations in the Caspian Sea*, Oceanology, Vol.57, p.360–375.

27- Perrone, T.J., (1979), *Winter shamal in the Persian Gulf. Monterey, California*, technical report, Naval Environmental Prediction Research Facility, I.R.-79-06, p.180.

28- Weggel, J., (1972), *Maximum breaker height for design*, In: Proceedings of the 13th International Conference on Coastal Engineering, Vancouver, Canada, ASCE, p. 419–432.

29- McCowan, J., (1894), *On the highest wave of permanent type*, The London, Edinburgh, and Dublin Philosophical Magazine and Journal of Science, Vol.5, p.351–358.

30- Dean, R. G. and Dalrymple, R. A., (1991), *Water Wave Mechanics for Engineers and Scientists*, World Scientific, Singapore.

31- Sunamura, T., (1984), *Quantitative predictions of beach-face slopes*, Geological Society of America Bulletin, Vol.95, p.242–245.